Stanford Exploration Project, Report 84, May 9, 2001, pages 1–50

Migration from a non-flat datum via reverse-time extrapolation

Gopal Palacharla[1]

ABSTRACT

Land surveys usually have elevation changes, and this irregular topography distorts seismic data. For large topography changes and near-surface velocity comparable to subsurface velocity, static-corrections are inadequate, wavefield extrapolation is required in this situation. I present a scheme for doing migration directly from the irregular datum. The scheme can also be used for redatuming data collected at a non-flat datum to a flat datum. The reverse-time migration method is used to do the extrapolation, because it is a boundary-value problem, which naturally accommodates an irregular topography. It can handle steep dips and a general velocity model. After describing the reverse-time algorithm, I apply it to a post-stack example and show that static shifts are inadequate but migration from a non-flat datum produces a good image. I also outline the shot-profile implementation and its extension to 3-D.

INTRODUCTION

Seismic data acquired in mountainous regions are distorted because of topography. Static corrections are inadequate when the elevation changes are steep and the near-surface velocity is high, since in this case the energy does not travel vertically. In this situation, wave-equation extrapolation is more appropriate than static shift. The standard, optimized migration algorithms assume the data is recorded on a flat surface. However, when there is substantial topography migration from the irregular datum should provide an accurate image. Several wavefield extrapolation methods are commonly used for migration, namely finite-difference methods, Kirchhoff methods, $f-k$ methods and reverse-time migration methods. For datuming, Berryhill (1979; 1984) applied the Kirchhoff integral method to wavefield extrapolation. The method is accurate and easy to implement for constant velocity. For variable velocity medium, however, the method encounters problems associated with an approximate solution to the wave equation and problems of ray tracing in complex media. Shtivelman and Canning (1988) have presented a Kirchhoff integral scheme similar to Berryhill. Bevc (1992) implemented the datuming scheme outlined by Berryhill and designed an anti-aliased operator. McMechan and Chen (1990) and Reshef (1991), have outlined approaches to do depth migration from irregular surfaces and McMechan and Chen incorporate receiver and source

[1]**email:** gopal@sep.stanford.edu

statics implicitly using reverse-time migration done via finite-differences. Reshef has presented a technique that allows extrapolation in depth from an irregular datum using downward continuation technique. Popovici (1992) applied phase-shift plus interpolation (PSPI) to perform datuming. Ji and Claerbout (1992) applied phase-shift method for datuming, but this method has difficulty in implementing lateral velocity variations. I present a migration algorithm that can handle data collected at an irregular surface, and it is based on the extrapolation of the scalar one-way acoustic wave equation via reverse-time method. I use a pseudo-spectral approach to do reverse-time migration. The reverse-time migration method has the advantage of handling the topography naturally, since it is a boundary value method. The method can also be used for redatuming the data collected at an irregular surface to a flat datum. Once the data have been redatumed a faster migration routine could be used to do the imaging. Using synthetic data, I show that static shift is inadequate, but migration from the irregular datum produces an accurate image. Finally, I outline the implementation for shot-profiles and 3-D post-stack data. The method can handle a general velocity medium and has the ability to handle steep dips. The routines for 2-D and 3-D zero-offset modeling and migration and 2-D shot-profile migration were implemented on the Connection Machine CM-5.

NUMERICAL IMPLEMENTATION

The derivation of the reverse-time migration algorithm starts with the one-way scalar wave equation

$$\pm\left[\frac{\partial^2}{\partial x^2}+\frac{\partial^2}{\partial y^2}+\frac{\partial^2}{\partial z^2}\right]^{\frac{1}{2}} p = \frac{1}{v(x,y,z)}\frac{\partial p}{\partial t}, \tag{1}$$

where $p = p(x,y,z,t)$ is the pressure field and $v = v(x,y,z)$ is the earth velocity. This wave equation is used in extrapolation. It is solved by a pseudo-spectral method. The time-differencing scheme is based on a third-order Taylor series expansion (Gazdag, 1981):

$$p(t+\Delta t) = p(t)+\frac{\partial p}{\partial t}\Delta t+\frac{\partial^2 p}{\partial t^2}\frac{\Delta t^2}{2!}+\frac{\partial^3 p}{\partial t^3}\frac{\Delta t^3}{3!}. \tag{2}$$

This is used for forward modeling. The synthetic data used in this paper were created using the above scheme. The migration equation, in which waves propagate backward in time, is given by

$$p(t-\Delta t) = p(t)-\frac{\partial p}{\partial t}\Delta t+\frac{\partial^2 p}{\partial t^2}\frac{\Delta t^2}{2!}-\frac{\partial^3 p}{\partial t^3}\frac{\Delta t^3}{3!}. \tag{3}$$

The time derivatives $\partial p/\partial t$ are evaluated by solving the wave-equation in the wavenumber domain,

$$\frac{\partial p}{\partial t} = \frac{v}{2}\left\{F^{-1} i\ sgn(k_z)\left[{k_x}^2+{k_y}^2+{k_z}^2\right]^{\frac{1}{2}} F\right\} p \tag{4}$$

where F and F^{-1} are operators representing the 3-D Fourier transform from the (x,y,z) domain to the (k_x,k_y,k_z) domain and its inverse. The sign of k_z, determines whether we are dealing with upcoming waves or downgoing waves. Downgoing waves are obtained using the plus sign and upcoming waves by the minus sign. Other more efficient time-differencing schemes (Tal-Ezer et al., 1987) can also be used for carrying out the extrapolation. Non-reflecting boundary conditions (Cerjan et al., 1985) are used on the sides and the bottom of the numerical mesh to avoid wraparound effects from the boundaries. Using the above scheme, the code for zero-offset modeling, zero-offset migration in 2-D and 3-D and 2-D shot-profile migration were developed and implemented on the Connection machine CM-5.

STABILITY AND ACCURACY

As with any wave-propagation simulation problem on a computational grid, the effect of the grid sampling and the medium characteristics on the accuracy and stability of the numerical scheme need to be studied. Since the space derivatives are evaluated in the Fourier domain, a sampling of 2 gridpoints/wavelength is sufficient for representing the Nyquist frequency This gives us a limit on the grid sampling based on aliasing:

$$\Delta x \leq \frac{v \Delta t_p}{2}, \tag{5}$$

where Δx is the grid sampling, Δt_p is the length of source pulse, and v is the velocity in the medium. The time-differencing which is based on a Taylor's series expansion, has a truncation error that leads to a phase and amplitude error, This error can be expressed in terms of a dimensionless quantity θ, given by

$$\theta = v \left[k_x^2 + k_z^2\right]^{\frac{1}{2}} \Delta t, \tag{6}$$

where k_x and k_z are the wavenumbers along x and z, and Δt is the computational time sampling. The differencing error is

$$\epsilon(\Delta t) = -\sum_{l=4}^{\infty} \frac{\partial^l p(t)}{\partial t^l} \frac{(\Delta t)^l}{l!}. \tag{7}$$

For a pure sinusoidal wave, $p = exp[i(k_x x + k_z z)]$, in a constant velocity medium the differencing error simplifies to

$$\epsilon(\theta) = -\sum_{l=4}^{\infty} \frac{(i\theta)^l}{l!}. \tag{8}$$

Gazdag (1981) plotted θ vs ϵ and found that the scheme was stable up to a $\theta \simeq 99\ degrees$. This gives a stability criterion of

$$\frac{v \Delta t_c}{\Delta x} \leq \alpha, \tag{9}$$

where α= 99/180 $\simeq$ 0.55 for plane waves. Putting the two limits together, leads to an inequality, which is given by

$$\frac{2\Delta x}{\Delta t_p} \leq v \leq \alpha \frac{\Delta x}{\Delta t_c} \tag{10}$$

Since v is defined by the subsurface, and Δx is the bin spacing which appears on both sides of the inequality, the parameter that could be changed to satisfy the inequality is t_c, the computational time sample. The inequality puts different limits on post-stack and shot-profile extrapolations, since the velocity used in post-stack implementation is half the earth velocity.

WAVEFIELD EXTRAPOLATION

post-stack implementation

The migration from non-flat datum, should be implemented in the shot-profile domain, rather than the post-stack domain, because it is difficult to obtain a stacked section when the data is distorted by topography. However I show a post-stack example because it is a first step in gaining intuition into the problems encountered with non-flat topography. I outline the shot-profile implementation in the next section. Reverse time migration of zero-offset data can be thought of as the process of taking the recorded zero-offset or exploding reflector experiment, and back propagating this wavefield back into the earth until time equals zero, the time the "exploding reflectors" explode. Reverse time migration proceeds by using time slices starting from the last time sample of the stacked data and going towards the first time sample (t=0) of the stacked section as a boundary condition for wave propagation in the specified velocity model. The computation scheme can be summarized with the help of the schematic in Figure **??**. Start with an all-zero (x,z) plane at the bottom of the data cube and extrapolate backward in time toward $t = 0$ to compute snapshots of the (x,z) plane at different times. These snapshots of the subsurface are indicated by the horizontal planes. The direction of extrapolation for migration is shown on the right. At each time level include the boundary value (x slice at $z = 0$, for flat datum, and x slice at $z = ztopo$ for a non-flat datum, indicated by the dotted line in the Figure **??**) into the (x,z) plane from the seismic section. The migrated section is the (x,z) plane at $t = 0$. The extrapolation is done via Equation 3. Figure **??** and Figure **??** show the vertical and horizontal sections of the impulse response of the 3-D reverse-time migration algorithm The parameters are $v = 2000m/s$, $dx = dy = dz = 12.5m$, $dt = 4ms$. The response is close to a hemi-sphere, indicating its ability to handle high dips. Modeling proceeds forward in time. It starts with a reflectivity model at time zero, and the snapshots are computed for forward time propagation. At each time step the data are extracted from the snapshot, it is the x-slice corresponding to $z = 0$ for a flat datum. For a non-flat datum the data is extracted along z defined by the topography z=$ztopo$. The method outlined in this paper can also be used to carry out datuming of the wavefield recorded at an irregular surface, to a flat surface above the recording surface using a constant velocity as suggested by Bevc (1992). This procedure enables velocity analysis of the data by removing the distortions caused by topography. The datuming to an upward datum can be performed by, forward time extrapolation, and at each time step I include the data ($x - slice$) corresponding to the data recorded at that time at the lower datum. For each time step, extract the data at the upper flat datum. The forward extrapolation is run for a time greater than the recorded time at the lower datum. Once the data has been datumed to a flat surface, a faster and efficient algorithm maybe

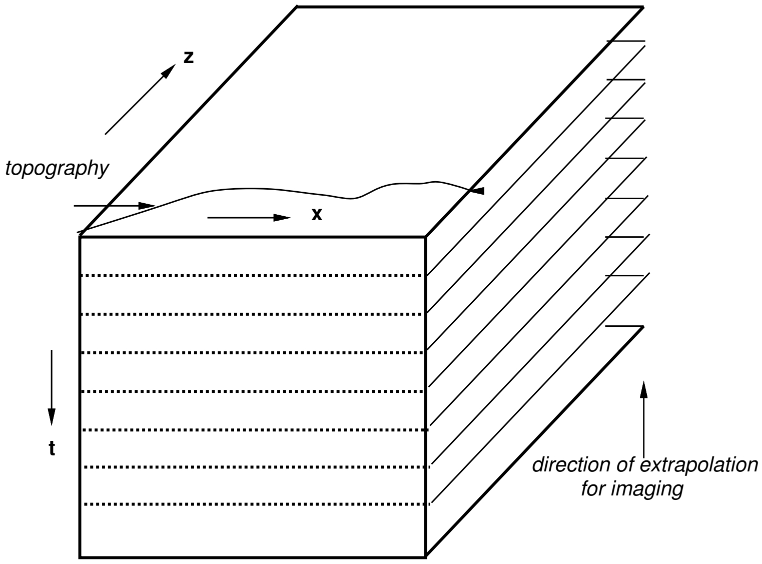

Figure 1: Schematic of reverse-time extrapolation. The scheme starts with an all zero horizontal plane at the bottom of the cube and extrapolates backward in time, towards $t = 0$. At each time level, the $x - slice$ corresponding to $z = 0$ or $z = ztopo$ is included in the extrapolation. The final migrated image is obtained at t=0. gopal1-scheme [NR]

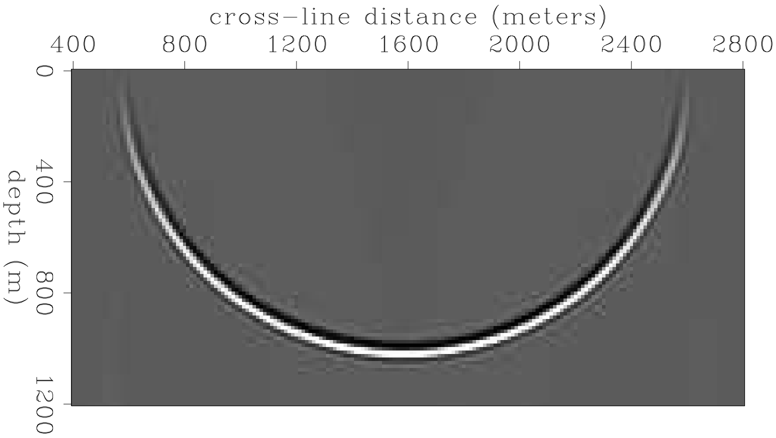

Figure 2: Vertical section from the impulse response of the 3-D reverse-time extrapolation scheme. The operator has a high-dip accuracy. gopal1-mig [CR]

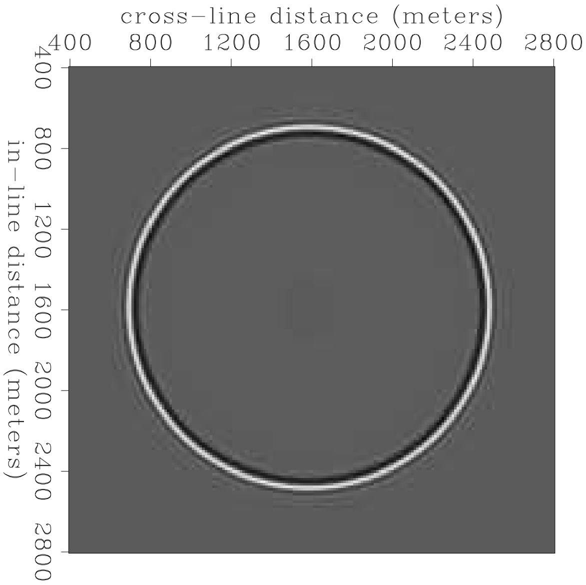

Figure 3: Depth slice from the 3-D reverse-time extrapolation operator. gopal1-threed [CR]

used for doing the migration.

Shot Profile Implementation

The shot-profile wavefield imaging consists of three steps, forward propagation of the shot wavefield, reverse propagation of receiver wavefield, and, finally, implementing the imaging condition. The shot wavefield is modeled using the differencing scheme in Equation 2. For a non-flat topography, the shot wavefield is computed from the actual source position. The receiver wavefield is backpropagated using the differencing scheme in Equation 3. For a non-flat topography, the recorded wavefield is backpropagated from the actual receiver positions (the implementation is the same as the zero-offset case shown in the previous section, except that the true velocity is used instead of half velocity), in a velocity model and it is imaged by measuring its amplitude when it is coincident with the primary shot wavefield. For shot-profile migration, the imaging condition is the time the shot wavefield takes to impinge on some boundary in the earth. At each time-step, the source and receiver wavefields are multiplied together at each grid point and the result is added to an image plane. The image plane is summed over all the time steps. This is equivalent to a zero-lag cross-correlation imaging condition. The shot wavefield is propagated from the shot point past all the reflecting horizons of interest; this occurs forward in time. The wavefield at each time step is written out to disk. Once this is done, the recorded wavefield is propagated back towards the reflectors using the one-way wave equation, this is done backward in time. When the recorded wavefield is at the same instant of time as the forward propagated shot, the image plane starts building up. Thus the two wavefields are multiplied together and added to the result of previous time levels to extract the position of the reflectors. This proceeds until time equals zero, when all of the reflected waves have been backpropagated into the model and have imaged the shot. The procedure can be extended to 3-D shot profiles in a straightforward manner. However, it is expensive in comparison to a Kirchhoff scheme. I have implemented a 3-D post-stack algorithm on the connection machine CM-5, using the Fast Fourier Transforms of the CM library. Figure **??** shows the depth slice from an impulse response test. The operator is azimuthally isotropic. Figure **??** shows the vertical section through the migrated cube. The size of the migrated cube is 256X256 surface grid and 128 depth samples. The trace spacing is 12.5 m and the velocity is 2000 m/s.

SYNTHETIC DATA EXAMPLES

I made a test model to study the responses of migration from a non-flat datum, migration of data after static correction, and compared the two results with that of the migration from a flat datum. Figure **??** shows the model along with the non-flat datum used in the study. There are

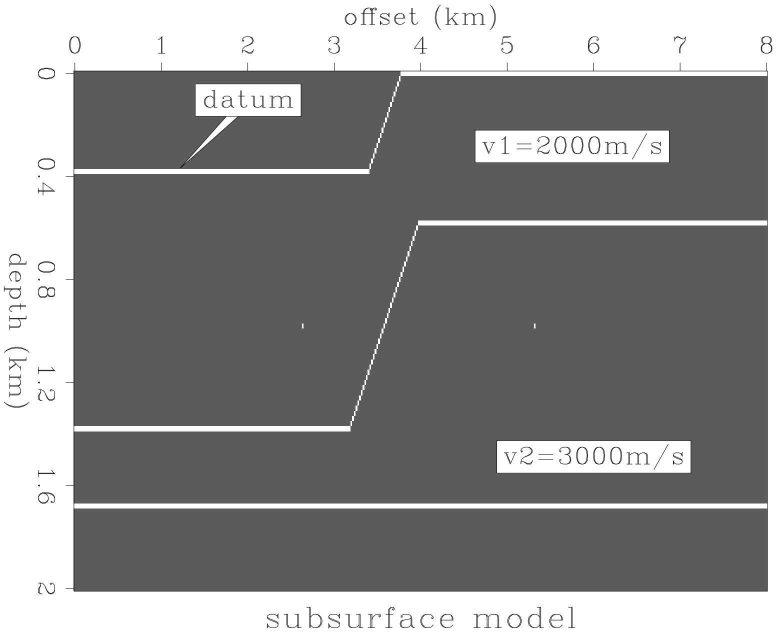

Figure 4: Model used in the numerical test. There are two scatterers on either side of the ramp. The velocity is 2km/s above the ramp and is 3km/s below. Two datasets were generated for this model: data as recorded at the surface z=0, data as recorded at the irregular datum. gopal1-datum [NR]

two diffractors on either side of the ramp-like feature. The slope of the ramp is 45 degrees. The non-flat datum has an elevation range of $400m$. The velocity varies from 2000 m/s to 3000m/s across the ramp. Two data sets are modeled; one was zero-offset data at the flat surface ($z = 0$) as shown in Figure **??**, and the second was zero-offset data at the non-flat datum (Figure **??**). The hyperbola on the left in Figure **??** now distorted because of topography. Figure **??** shows the data after static correction of the data modeled at the non-flat datum. Next, the three datasets were migrated. Figure **??** shows the migration of the data from flat-datum. The events have been imaged at their proper positions. Figure **??** shows the migration of the data collected at the non-flat datum. The events in this case have also been moved to their correct position. The diffractor on the left has some artifacts. Figure **??** shows the migration result

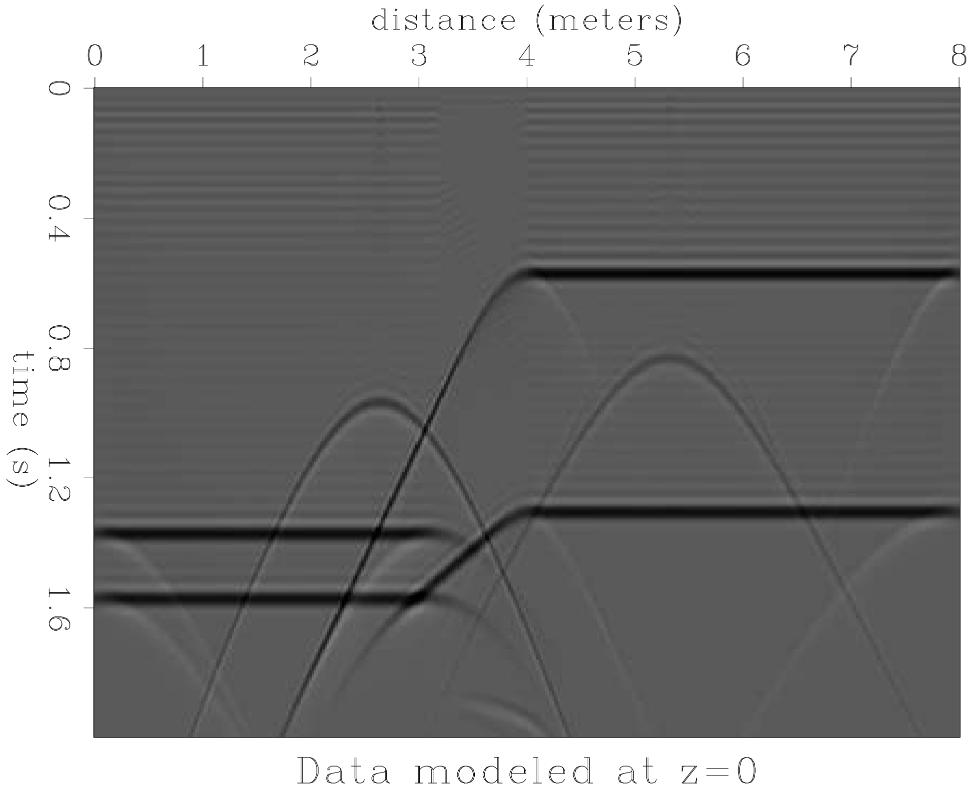

Figure 5: Data modeled at the flat datum (z=0). gopal1-flatdat [CR]

of static-corrected data. The diffractor on the left is not completely focused, also the ramp has shifted to the right. This can be explained by the fact, that zero-offset rays from the slope travel at 45 degrees, whereas the static-shift is applying a vertical correction. Figure **??** shows the data after upward datuming to a flat datum of the data modeled at the lower non-flat datum. Compare this with Figure **??** which shows the data modeled at the flat surface. The distortion due to the topography has been removed.

DISCUSSION AND CONCLUSIONS

The schemes presented here require a reliable estimate of the near-surface velocity, which needs to be obtained by refraction statics analysis or by doing a tomographic inversion for the velocity distribution (Zhu and McMechan, 1988). The datuming algorithm can be used to extrapolate the data upwards to a flat datum assuming a velocity. This eliminates the distortions caused by irregular topography. We can perform velocity analysis at the flat datum to determine the near-surface velocity structure as suggested by Bevc (1992). I developed a scheme for zero-offset modeling, zero-offset migration, and shot-profile migration that were capable of handling irregular topography and preserving steep dips. Receiver elevation corrections are incorporated by extrapolating the recorded data from the actual receiver positions, and source elevation is accounted for by computing the excitation time from the actual source position.

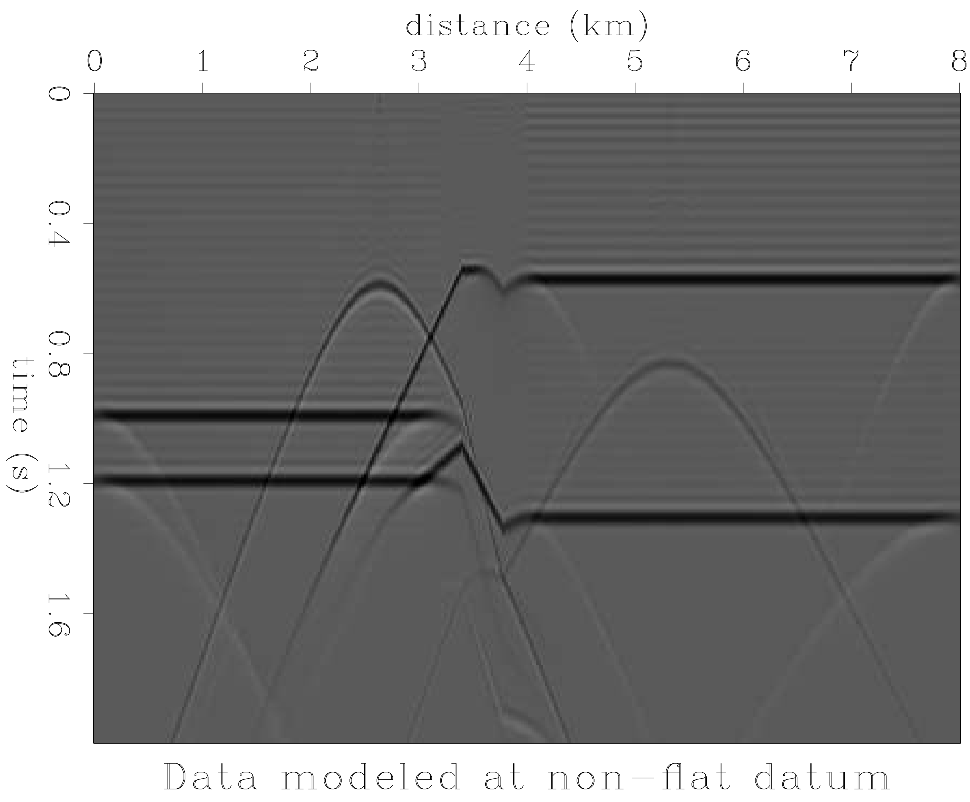

Figure 6: Data modeled at the non-flat datum that is indicated in Figure 4. The two hyperbolas are distorted as expected. gopal1-irrdat [CR]

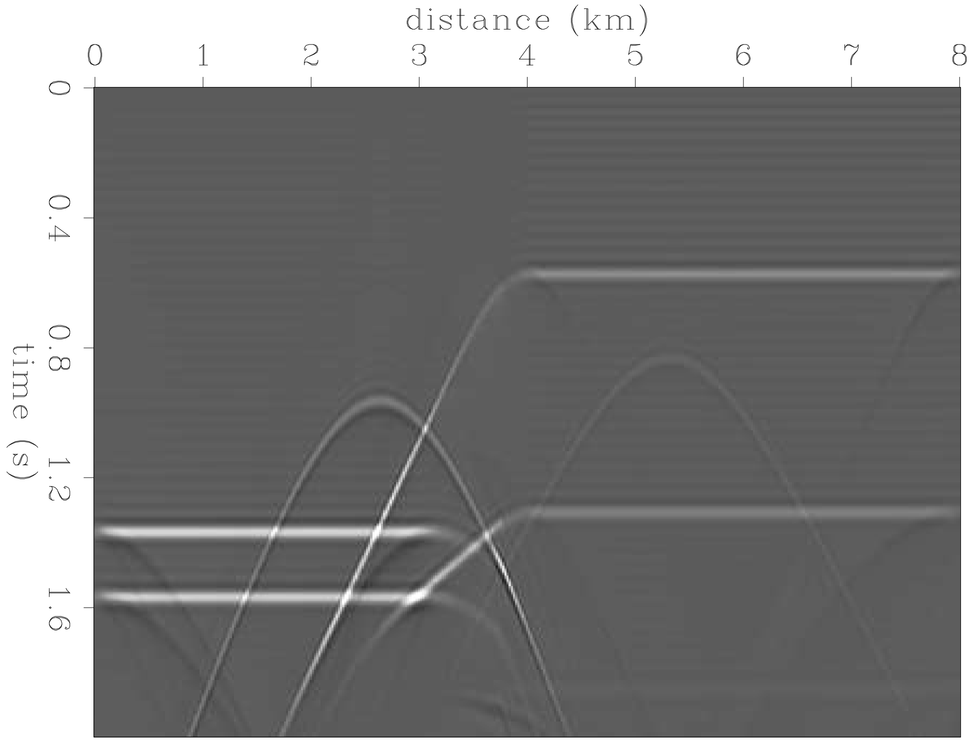

Figure 7: Data after continuation to the surface z=0, of the data collected at the non-flat datum. Compare with Figure 5. gopal1-datmup [CR]

Static shift is shown to be inappropriate but migration from non-flat datum produces accurate images. The algorithm can be used to migrate the data directly from the flat datum, or the method can also be used to extrapolate the data to a flat datum, and a faster imaging algorithm can be used for the migration. The algorithm has high dip accuracy and can handle lateral velocity variations.

ACKNOWLEDGEMENTS

This research started during my summer internship at Exxon Production Research Company. I would like to thank Dr. Y. C. Kim of Exxon for his comments and discussions.

REFERENCES

Berryhill, J. R., 1979, Wave equation datuming: Geophysics, **44**, no. 8, 1329–1344.

Berryhill, J. R., 1984, Wave equation datuming before stack (short note): Geophysics, **49**, no. 11, 2064–2067.

Bevc, D., 1992, Kirchhoff wave-equation datuming with irregular acquisition topography: SEP–**75**, 137–156.

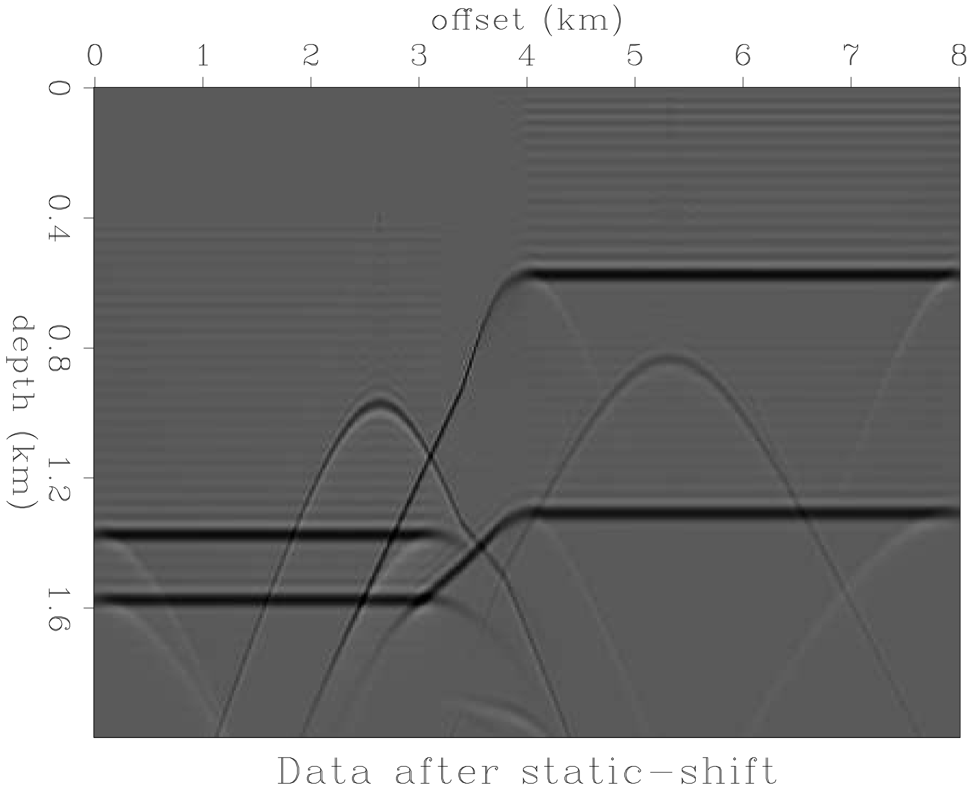

Figure 8: Data at the surface after static shifting the non-flat datum data. gopal1-shifdat [CR]

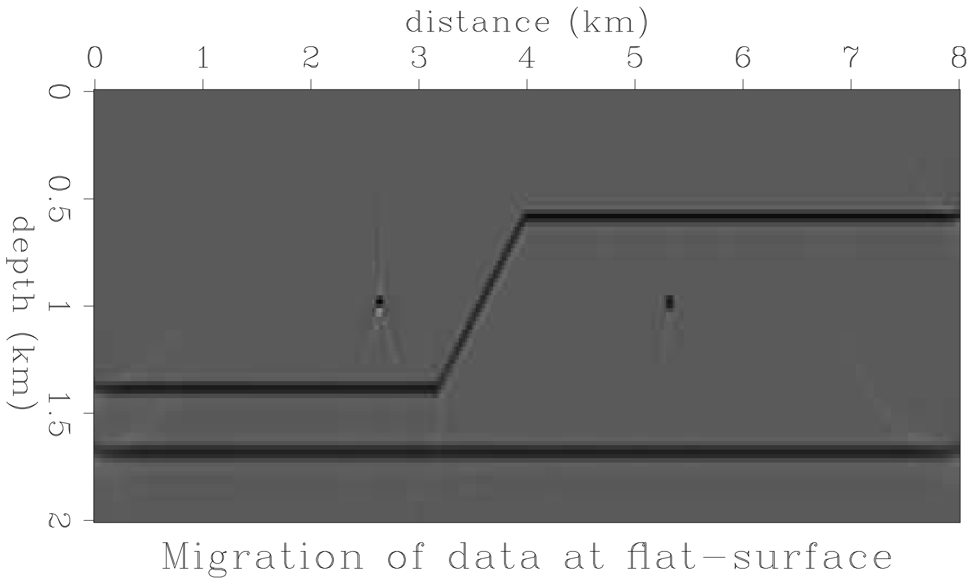

Figure 9: Migration of the data collected at the flat surface. The events are well imaged. gopal1-migflat [CR]

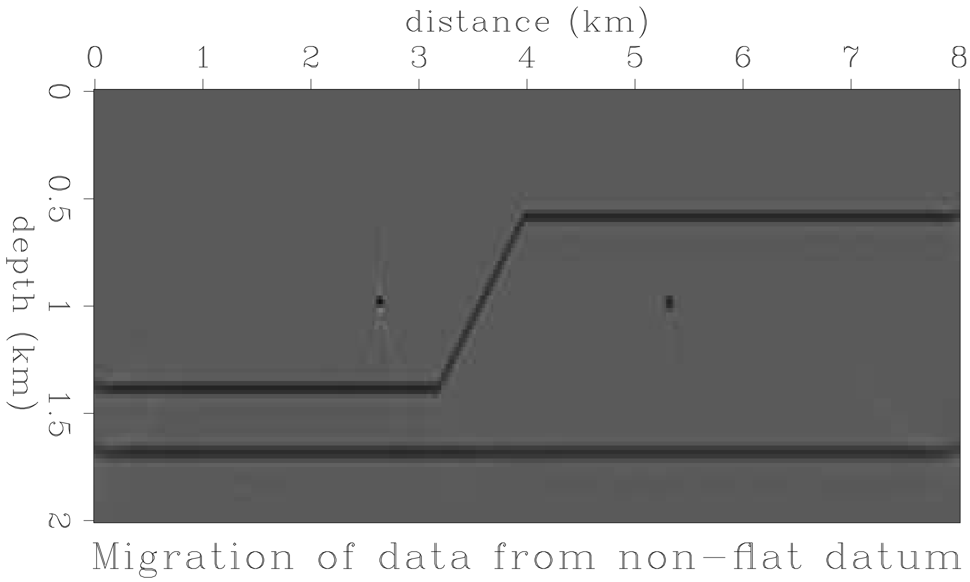

Figure 10: Migration of the data collected at the non-flat datum. The events are well imaged. gopal1-irrmig [CR]

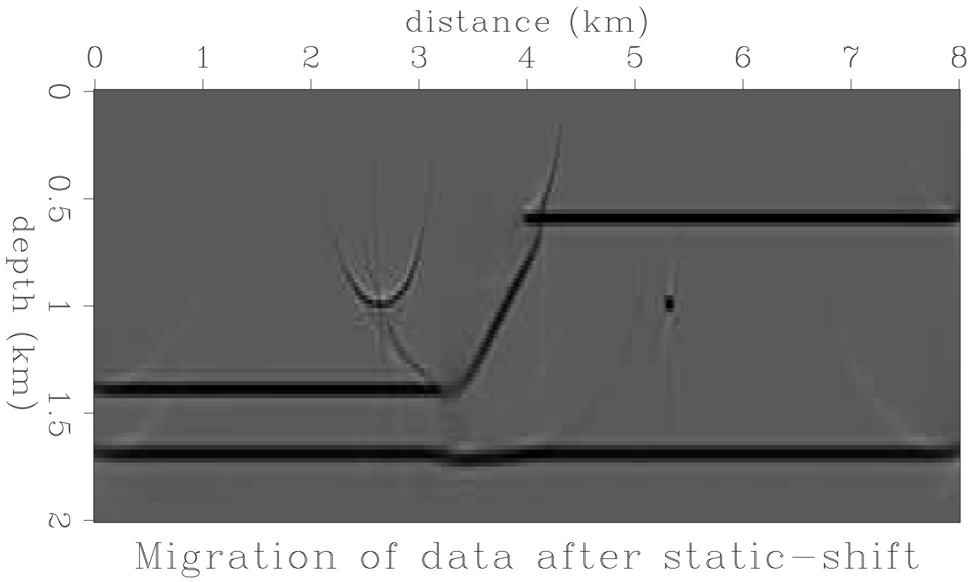

Figure 11: Migration of the data after static shift. As expected, the image is distorted since the static shift does not account for ray bending. gopal1-migshif [CR]

Cerjan, C., Kosloff, D., Kosloff, R., and Reshef, M., 1985, A nonreflecting boundary condition for discrete acoustic-wave and elastic-wave equations (short note): Geophysics, **50**, no. 4, 705–708.

Gazdag, J., 1981, Modeling of the acoustic wave equation with transform methods: Geophysics, **46**, no. 6, 854–859.

Ji, J., and Claerbout, J., 1992, Phase shift datuming and migration from an irregular surface: SEP–**75**, 157–170.

McMechan, G. A., and Chen, H. W., 1990, Implicit static corrections in prestack migration of common-source data: Geophysics, **55**, no. 6, 757–760.

Popovici, M., 1992, Wave-equation datuming in variable velocity media: SEP–**75**, 191–214.

Reshef, M., 1991, Depth migration from irregular surfaces with depth extrapolation methods: SHORT NOTE: Geophysics, **56**, no. 1, 119–122.

Shtivelman, V., and Canning, A., 1988, Datum correction by wave equation extrapolation: Geophysics, **53**, no. 10, 1311–1322.

Tal-Ezer, H., Kosloff, D., and Koren, Z., 1987, An accurate scheme for seismic forward modeling: Geophys. Prosp., **35**, no. 5, 479–490.

Zhu, X., and McMechan, G. A., 1988, Estimation of near surface velocities by tomography: Estimation of near surface velocities by tomography:, Soc. Explor. Geophys., 58th Ann. Internat. Mtg., Soc. Explor. Geophys.,Expanded Abstracts, 1236–1238.